Presented at the 17th Workshop on Crystalline Silicon Solar Cells & Modules: Materials and Processes (Vail Cascade Resort, Vail, CO, Aug. 5 – 8, 2007).

Effect of Surface Passivation on Si Heterojunction and Interdigitated Back Contact Solar Cells

U. K. Das, S. Bowden, M. Burrows, M. Lu, and R. W. Birkmire
Institute of Energy Conversion, University of Delaware, 451 Wyoming Rd, Newark, DE 19716, USA

Abstract

Silicon surface passivation of hydrogenated silicon (Si:H) thin films deposited by RF and DC plasma process was investigated by measuring effective minority carrier lifetime (τ_{eff}) on Si <100> and <111> wafers and correlated with the silicon heterojunction (SHJ) cell performances in front emitter structure and interdigitated back contact (IBC) structure. Excellent surface passivation (τ_{eff} > 1 msec) and high efficiency front emitter SHJ cells are obtained by both RF and DC plasma deposited intrinsic a-Si:H buffer layer. High efficiency with open circuit voltage (V_{OC}) of 694 mV was achieved on n-type textured Cz wafer using DC plasma deposited buffer layer. High V_{OC} of 683 mV is also achieved in an exploratory IBC heterojunction structure and needs further optimization for improved fill factor.

Introduction

Fabrication of crystalline silicon (c-Si) heterojunction (SHJ) devices by the deposition of wide band gap semiconductors such as amorphous hydrogenated silicon (a-Si:H) are a demonstrated way to fabricate high efficiency c-Si solar cells [1-3]. High efficiency of a-Si:H/c-Si SHJ solar cells is primarily due to increased open circuit voltages (V_{OC}). The increase in V_{OC} is achieved by reduced surface recombination and low emitter saturation currents using a thin intrinsic a-Si:H buffer (i-layer) on both surfaces of c-Si wafer. However, the a-Si:H layer absorbs short wavelength (<600 nm) light and the best passivation is achieved with thicker layers, resulting in greater absorption losses and reduced short circuit currents (J_{SC}) in the front emitter SHJ cells. Formation of heterojunction with both a-Si:H emitter and base contact on the back side in an interdigitated pattern would hence improve the cell blue response and J_{SC} and offer a pathway to realize the full potential of heterojunction devices. Furthermore, a good front surface passivation quality is absolutely necessary for interdigitated back contact (IBC) structure, since the carriers that are generated near the front surface need to diffuse the entire wafer thickness to be collected in the rear.

In this work, we studied the surface passivation quality of a-Si:H i-layers deposited with varying hydrogen dilution on n-type float zone (FZ) Si wafers with two different crystallographic orientation (<100> and <111>) and correlate with the device performances of front emitter SHJ and IBC cells. The SHJ cells were also fabricated on n-type textured Czochralski (Cz) Si wafers, where <100> surface changes to <111> after texturing to realize the benefit of light scattering. Additionally, the a-Si:H layers were deposited by standard 13.56 MHz RF plasma and by DC glow discharge process. Comparison between the two processes elucidates the effect of ion bombardment on Si surface passivation and cell performances during growth of these thin layers.

Experimental

The n-type Si wafers (~300 μm) with resistivity of 1.0 Ω.cm for <100> and 2.5 Ω.cm for <111> were cleaned for 5 mins in a mixture of H_2SO_4:H_2O_2 (4:1) followed by 5 mins rinse in de-ionized water and in 10% HF for 30 sec prior to each Si:H deposition. The Si:H i-layers (10 nm) were deposited on both sides by RF and DC plasma process using a six-chamber large area (30 × 35 cm²) deposition system. The substrate temperature, deposition pressure and SiH_4 flow rate were fixed at 200°C, 1250 mTorr and 20 sccm respectively. The primary variable in i-layer process is the H_2 flow rate, which was varied from 0 to 200 sccm and characterized by the dilution ratio R = H_2/SiH_4. The RF power of 30 W and a DC plasma current of 123 mA were maintained constant. The quality of surface passivation was determined by measuring effective minority carrier lifetime (τ_{eff}) using photoconductive decay method [4]. Thin layers

(10 nm) of p-type a-Si:H emitter followed by 70 nm Indium Tin Oxide (ITO) with metal grids in the front and n-type a-Si:H followed by evaporated Al contact on the rear were deposited to fabricate front emitter SHJ cells. The interdigitated pattern of deposited p- and n-type a-Si:H layers (20 nm) and evaporated Al contacts were created for IBC structure by two step photolithography processing, where the p-region has lateral dimension of 1.2 mm and n-region is 0.5 mm wide. The front surface of IBC cells were passivated by a 20 nm a-Si:H i-layer followed by antireflection (AR) coatings composed of ITO and MgF_2 layers. This surface passivation/AR structure is not ideal for high J_{SC} but provided a means of evaluating the device performance and the utility of the structure as an alternate diagnostic tool to evaluate surface recombination.

Results and Discussions

Figure 1 shows the τ_{eff} as a function of R for i-layers deposited on <100> and <111> wafers by DC and RF plasma after annealing the samples at 280°C for 10 mins. It is worth noting that the DC plasma process will have a significantly higher ion bombardment compared to RF in otherwise similar plasma parameters due to higher plasma potential. Three distinct regions can be identified in the variation of τ_{eff} with R (Fig. 1). In region I (R < 2), τ_{eff} shows plasma process dependence, namely, DC plasma deposited i-layer at R = 0 show lower lifetime (~ 500 μsec) compared to RF plasma deposited i-layers (> 1 msec) irrespective of the surface orientation. With R = 0 at 1250 mTorr, it is likely to have significant poly-silane contribution in the film deposition for both DC and RF plasma with comparatively higher in DC due to larger amount of ionic species, resulting in a more defective film in DC process, thereby reduces τ_{eff}. Formation of poly-silane decreases with an increase of R in DC plasma [5] and improves film quality. Hence, τ_{eff} becomes similar for both RF and DC plasma deposited i-layers at R > 2 (region II and III in Fig.1), implying little / no deleterious effect of ion damage in DC process on Si surface passivation.

In region III (R > 4), however, the measured τ_{eff} exhibits a pronounced Si surface orientation dependence. The values of τ_{eff} sharply decreases to < 10 μsec on <100> wafers for i-layers deposited with R > 4, while on <111> wafers remains > 1 msec even at R = 10 for both RF and DC process. It was found out from variable angle spectroscopic ellipsometry (VASE) measurement that i-layer at R > 4 on <100> wafers grow epitaxial or nanocrystalline, while the films remain amorphous on <111> wafers. Low value of τ_{eff} and loss of surface passivation on <100> wafers by R > 4 i-layers are likely due to the low band gap of epitaxial or nanocrystalline Si layers with larger amount of defects at the interface.

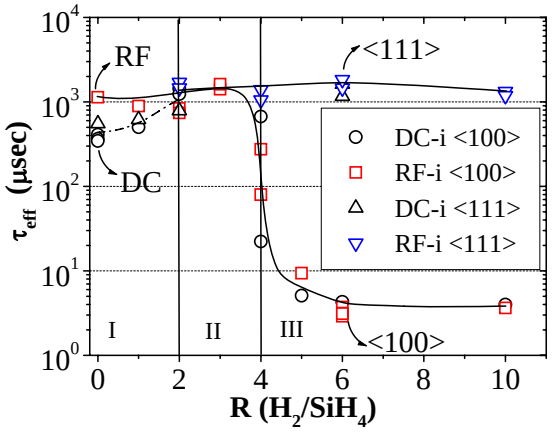

Figure 1: Effective minority carrier lifetime (τ_{eff}) on Si <100> and <111> wafers with 10 nm Si:H i-layer deposited on both sides by RF and DC plasma at varying hydrogen dilution (R). The lines are guide to the eyes.

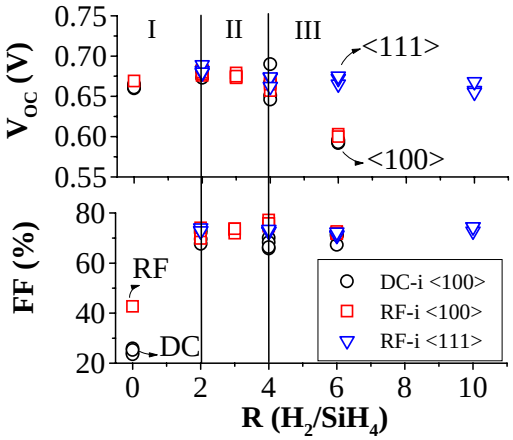

Figure 2: Open circuit voltage (V_{OC}) and fill factor (FF) of SHJ cells on Si <100> and <111> wafers with i-layers deposited by RF and DC plasma process at different hydrogen dilution (R).

After completion of lifetime testing of all the samples, they were converted into front emitter SHJ cells by depositing p- and n-type a-Si:H including the ITO and metal contacts. The J_{SC} values were rather similar for all the devices, while the cell efficiency changes with R in i-layers due to changes in V_{OC} and FF. Figure 2 shows the variation of V_{OC} and fill factor (FF) of the cells as a function of R for i-layers deposited on <100> by DC and on both <100> and <111> wafers by RF plasma. Interestingly, the V_{OC} exhibits pronounced wafer orientation dependence in region III (R = 6), while FF exhibits only plasma process dependence in region I (R = 0). The cell V_{OC} correlates well to the variation of τ_{eff} with R as shown in Fig.1, and decreases to ~ 600 mV for the i-layer deposited with R = 6, demonstrating the necessity of high τ_{eff} and good surface passivation quality to achieve high V_{OC}. However, high value of τ_{eff} alone does not insure a high efficiency device because the FF decreases drastically to < 50% with an "S" shape J-V for the i-layers grown at R = 0, despite exhibiting τ_{eff} of > 1 msec in RF process in Fig.1. The poly-silane contribution in the film growth at R = 0 forms a defective and presumably wider band gap layer with higher SiH_2 bonding for both processes with an enhanced effect in DC discharge. Such a defective and wide band gap a-Si:H film severely inhibits carrier transport across the i-layer, particularly the hole transport over a large valence band offset in the emitter side and reduces FF. On the other hand, epitaxial / nanocrystalline growth at R = 6 narrows the band gap of deposited layer and therefore does not affect hole transport and cell FF, but results in low V_{OC} due to insufficient surface passivation. Consequently, the highest SHJ cell efficiency was obtained for i-layers deposited with R = 2.

Table-I summarizes the best device performances on n-type polished FZ <100>, <111> and n-type textured Cz wafers with i-layers deposited by DC and RF processes. Both plasma processes demonstrate SHJ cells with high efficiency and high V_{OC}, therefore, seemingly higher ion bombardment in DC process have neither any effect on surface passivation nor in the cell performance. The SHJ cell efficiency of 18.8% with V_{OC} of 694 mV was achieved on textured Cz wafer due to efficient light scattering and additional MgF_2 AR layer in the front light illuminating surface.

Table-I: Summary of the best front emitter SHJ device performances on n-type polished FZ <100>, <111> and n-type textured Cz wafers with the i-layers deposited by both DC and RF processes.

Wafer	a-Si:H i-layer process	V_{OC} (V)	FF (%)	J_{SC} (mA/cm^2)	Efficiency (%); not independently confirmed
N – FZ<100>	DC	0.686	72.2	32.8	16.2
	RF	0.680	74.1	32.6	16.4
N – FZ<111>	RF	0.689	74.0	33.8	17.2
N – Tex. Cz	DC	0.689	74.0	35.0	17.8
N – Tex. Cz with additional MgF_2 AR coating	DC	0.694	74.4	36.4	18.8

The short wavelength quantum efficiency and hence the cell J_{SC} is expected to increase significantly for the IBC solar cell structure, since it allows independent control for optimum passivation with low reflection / absorption loss in the front illuminating surface and minimization of electrical series resistance in the rear. The IBC structure fabricated on n-type FZ <100> wafers in this work is, however, not optimized in the front surface. Instead, the front surface consists of 20 nm thick R2 a-Si:H i-layer (same total thickness of a-Si:H layer as front emitter SHJ cells) followed by alike AR coatings and thus provide similar optical layers in the front to allow a direct comparison of cell performances with front emitter SHJ cells. The rear side of IBC cells consists of two different structures; (i) interdigitated p- and n-strips without any i-layer [Figure 3(a)] and (ii) 8 nm R2 i-layer over the whole rear surface followed by interdigitated p- and n-strips [Figure 3(b)]. The dimensions of p- and n-strips in the two structures were identical, but width of the gap between p- and n-strip and surface passivation in rear was different. In case of no i-layer in the rear, about 2 μm gap was not passivated by any amorphous layer, while a wider gap of 50 μm along with the entire rear surface was passivated by i-layer in the second structure.

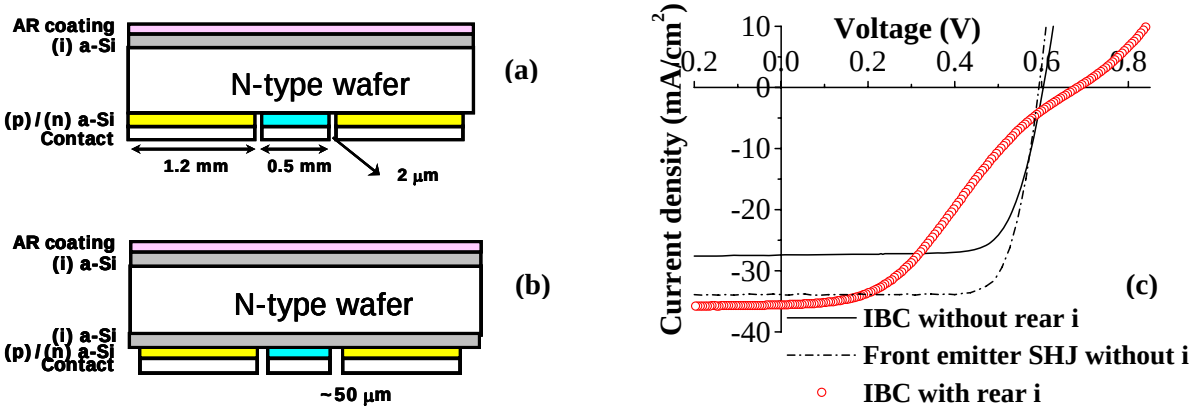

Figure 3: Schematic cross section of heterojunction cells in IBC structure (a) without i-layer passivation in the rear; (b) with i-layer passivation in the rear; and (c) Illuminated (AM 1.5) J-V for the IBC heterojunction cells, with and without rear i-layer and a front emitter SHJ cells without buffer i-layer.

Figure 3(c) compares the J-V curve under AM 1.5 illumination for the IBC cells with two structures and a front emitter SHJ cell without any i-layer. The figure clearly demonstrate that the V_{OC} and FF are identical for the cells without i-layer passivation in the emitter and contact side for both front emitter SHJ and IBC structure. However, J_{SC} of the IBC cell is ~ 6 mA/cm^2 lower than that of front emitter SHJ cell and achieved an independently confirmed efficiency of 11.8% in IBC heterojunction cell. An unpassivated gap between the emitter and contact strips acts as an efficient recombination region for the photogenerated carriers and reduces J_{SC} in IBC structure. Consequently, the IBC cell with the entire rear surface passivated by i-layer exhibits both increased J_{SC} and V_{OC}. The V_{OC} of 683 mV is similar to that of the front emitter SHJ cell on <100> wafer as shown in Table-I and indicative of good passivation in the emitter and contact strips but has a low FF. Such an "S"-shape J-V suggests existence of carrier transport barrier across i-layers and requires separate optimization of the layer in the IBC structure.

Conclusions

In conclusion, excellent surface passivation (τ_{eff} > 1 msec) and high V_{OC} in SHJ cells are achieved by both RF and DC plasma process with hydrogen dilution. Any epitaxial / nanocrystalline growth of i-layer reduces τ_{eff} and cell V_{OC}. The structure of deposited thin Si:H layers strongly depend on the Si substrate orientation. The front emitter SHJ cell efficiency approaching 19% with V_{OC} of 694 mV was achieved on textured Cz wafer using DC plasma deposited i-layer. The exploratory heterojunction cells in IBC structure reveals importance of surface passivation in the rear to achieve high V_{OC} (683 mV) and J_{SC} but demands further optimization of i-layer for improved carrier transport across it and cell FF.

Acknowledgment

The work was partly funded by BP Solar and partly by NREL under subcontract # ADJ-1-30630-12.

REFERENCES

[1] M. Taguchi, A. Terakawa, E. Maruyama, and M. Tanaka, Prog. Photovoltaics 13, 481 (2005).

[2] T. H. Wang, Q. Wang, E. Iwaniczko, M. R. Page, D. H. Levi, Y. Yan, C. W. Teplin, Y. Xu, X. Z. Wu, and H. M. Branz, Proceedings of the 19th European Photovoltaic Solar Energy Conference, Paris, France (2004), p. 1296.

[3] H. Fujiwara and M. Kondo, Appl. Phys. Lett. 90, 013503 (2007).

[4] S. Bowden, U. K. Das, S. S. Hegedus, and R. W. Birkmire, Proceedings of the 4th IEEE World Conference on Photovoltaic Energy Conversion, Hawaii, (2006), p. 1295.

[5] G. Ganguly, J. Newton, D. E. Carlson, and R. R. Arya, J. Non-Cryst. Solids 299–302, 53 (2002).